


An Embryonic and Induced Pluripotent Stem Cell Model for Ovarian Granulosa Cell Development and Steroidogenesis

Reproductive Sciences
2018, Vol. 25(5) 712-726
© The Author(s) 2017
Reprints and permission:
sagepub.com/journalsPermissions.nav
DOI: 10.1177/1933719117725814
journals.sagepub.com/home/rsx


Shane Lipskind, MD¹, Jennifer S. Lindsey, BS¹,
Behzad Gerami-Naini, PhD², Jennifer L. Eaton, MD²,
Daniel O'Connell, PhD², Adam Kiezun, PhD³,
Joshua W. K. Ho, PhD⁴, Nicholas Ng, BS¹, Parveen Parasar, DVM¹,
Michelle Ng, PhD¹, Michael Nickerson, BS¹, Utkan Demirci, PhD⁵,
Richard Maas, MD, PhD^{2,6}, and Raymond M. Anchan, MD, PhD^{1,6}

Abstract

Embryoid bodies (EBs) can serve as a system for evaluating pluripotency, cellular differentiation, and tissue morphogenesis. In this study, we use EBs derived from mouse embryonic stem cells (mESCs) and human amniocyte-derived induced pluripotent stem cells (hAdiPSCs) as a model for ovarian granulosa cell (GC) development and steroidogenic cell commitment. We demonstrated that spontaneously differentiated murine EBs (mEBs) and human EBs (hEBs) displayed ovarian GC markers, such as aromatase (CYP19A1), FOXL2, AMHR2, FSHR, and GJA1. Comparative microarray analysis identified both shared and unique gene expression between mEBs and the maturing mouse ovary. Gene sets related to gonadogenesis, lipid metabolism, and ovarian development were significantly overrepresented in EBs. Of the 29 genes, 15 that were differentially regulated in steroidogenic mEBs displayed temporal expression changes between embryonic, postnatal, and mature ovarian tissues by polymerase chain reaction. Importantly, both mEBs and hEBs were capable of gonadotropin-responsive estradiol (E2) synthesis in vitro (217-759 pg/mL). Live fluorescence-activated cell sorting-sorted AMHR2⁺ granulosa-like cells from mEBs continued to produce E2 after purification (15.3 pg/mL) and secreted significantly more E2 than AMHR2⁻ cells (8.6 pg/mL, $P < .05$). We conclude that spontaneously differentiated EBs of both mESC and hAdiPSC origin can serve as a biologically relevant model for ovarian GC differentiation and steroidogenic cell commitment. These cells should be further investigated for therapeutic uses, such as stem cell-based hormone replacement therapy and in vitro maturation of oocytes.

Keywords

embryonic stem cells, native hormones, ovarian tissue regeneration, steroidogenesis, iPSC

¹ Division of Reproductive Endocrinology and Infertility, Department of Obstetrics, Gynecology and Reproductive Medicine, Brigham and Women's Hospital and Harvard Medical School, Boston, MA, USA

² Division of Genetics, Department of Medicine, Brigham and Women's Hospital and Harvard Medical School, Boston, MA, USA

³ Computational Methods Development, Cancer Genome Analysis, Broad Institute of MIT and Harvard, Cambridge, MA, USA

⁴ Victor Chang Cardiac Research Institute, University of New South Wales, Sydney, New South Wales, Australia

⁵ Canary Center at Stanford for Early Cancer Detection, Stanford School of Medicine, Palo Alto, CA, USA

⁶ Affiliated Faculty, Harvard Stem Cell Institute, Cambridge, MA, USA. Gerami-Naini is now with the Department of Diagnostic Sciences, School of Dental Medicine, Tufts University, Boston MA, USA. Eaton is now with the Division of Reproductive Endocrinology and Fertility, Department of Obstetrics and Gynecology, Duke University School of Medicine, Durham, NC, USA. O'Connell is now with the Intellia Therapeutics, Inc, Cambridge, MA, USA. Kiezun is now with the Amazon.com, Boston, MA, USA

Corresponding Author:

Raymond M. Anchan, Department of Obstetrics, Gynecology and Reproductive Biology, Brigham and Women's Hospital, Center for Infertility and Reproductive Surgery, Harvard Medical School, 75 Francis Street, Boston, MA 02115, USA.

Email: ranchan@bwh.harvard.edu

Introduction

The female hypothalamic–pituitary–ovarian axis regulates ovarian folliculogenesis and sex steroid production. Premature loss of native ovarian sex steroid production can impact quality of life and overall health in many ways. For example, women with primary ovarian insufficiency (POI) may experience hot flashes, insomnia, decreased libido,^{1–4} cognitive changes,^{5,6} accelerated bone loss,^{7,8} and increased cardiovascular risk.⁹ Typically, women with symptomatic hypoestrogenemia are treated with hormone replacement therapy (HRT) using either equine or synthetic estrogens, alone or in combination with progestins. Due to concerns for increased risk of cardiovascular disease, venous thromboembolism,^{10,11} and breast cancer associated with conventional HRT,^{12–15} nonpharmacologic methods for restoring natural hormonal function warrant further consideration.

Embryonic stem cells (ESCs) and induced pluripotent stem cells (iPSCs) appear to hold significant promise in the fields of regenerative medicine, cell therapy, and tissue replacement. Several studies have sought to generate ovarian cell types from ESCs and iPSCs, yet it has been challenging to isolate functional oocytes and granulosa cells (GCs) capable of estradiol (E2) production from SCs.^{16–24} When grown in suspended culture, ESCs and iPSCs are known to form aggregates of differentiating cells called embryoid bodies (EBs). The EBs mimic embryonic development and have been used to examine tissue generation. Spontaneously differentiated human EBs (hEBs) have been shown to initiate sex steroid synthesis *in vitro* and produce E2- and progesterone (P4)-secreting cells.^{25–27} As such, this system can serve as a potential *in vitro* model for ovarian development that recapitulates *in vivo* ovarian development (Figure 1).

The purpose of this study was to determine whether spontaneously differentiated mEBs contain a purifiable subpopulation of stem cell–derived ovarian granulosa-like cells (SC-GCs) that display archetypal ovarian gene expression (*Cyp19a*, *Foxl2*, *Amhr2*, *Fshr*, and *Gja1*) and are capable of steroidogenesis. Furthermore, we hypothesized that there are shared gene regulatory pathways in the maturing mouse ovary (embryonic day 9 [E9], postnatal day 2 [P2], and adult mural GCs) and identified parallel transcriptional changes in this SC differentiation system. We present evidence that an SC model for ovarian GC differentiation, as characterized here, may provide valuable insights into ovarian development and ultimately allow the restoration of ovarian function via generation of native hormones or a biological matrix for *in vitro* oocyte development.

Materials and Methods

All supplies were purchased from Sigma Aldrich (St Louis, Missouri) unless otherwise noted. All experiments using animal tissue were performed with strict adherence to the approved Institutional Animal Care and Use Committee (IUCAC) protocol (#750, 05200).

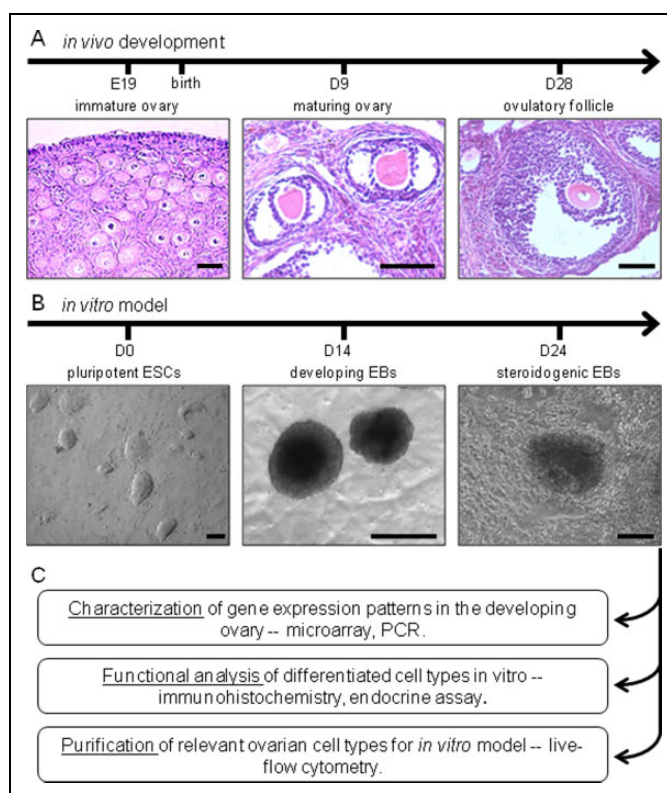


Figure 1. Experimental design comparing *in vivo* development of the ovary (A) with *in vitro* generation of EBs from mouse ESCs (B). The utility of this *in vitro* model is analyzed by examining EB gene expression patterns, steroidogenic functionality, and composition (C). Scale bars: (A) 50 μ m and (B) 100 μ m. EBs indicates embryoid bodies; ESCs, embryonic stem cells.

Processing of Ovarian Tissues

Control ovarian tissues were obtained from FVB mice (Jackson Laboratories, Bar Harbor, Maine), which were handled in accordance with our institutional policies and procedures. In this study, 8- to 12-week-old mice stimulated with equine chorionic gonadotropin (eCG) with or without 0.1 mg human chorionic gonadotropin were killed for ovarian harvesting. Mural GC isolation was achieved using laser capture microdissection (laser capture microscopy [LCM], described below). Mural GC sections were pooled for RNA extraction and reverse transcription polymerase chain reaction (RT-PCR). Stimulated adult ovaries were used for sectioning and immunocytochemistry (ICC), as well as RNA extraction. For sectioning, adult ovaries were immediately fixed with cold 4% paraformaldehyde/4% sucrose and embedded in paraffin, per standard protocol. RNA was extracted using commercially available kits (Qiagen, Germantown, Maryland) and extraction quality was analyzed using a Nanodrop 2000 (Nanodrop, Wilmington, Delaware). Expression of ovarian and GC developmental markers was assessed with commercially available kits for RT of complementary DNA (cDNA; Quanta Biosciences, Gaithersburg, Maryland) and PCR (Promega, Madison, Wisconsin). The PCR products were separated via gel electrophoresis (Bio-Rad, Hercules, California) to determine the presence or absence of expression.

Immature mouse ovaries were obtained from P2 pups. Mouse embryonic ovarian tissue was obtained from caudal dissections of E9 and E17 fetuses. These tissues were pooled and homogenized for RNA extraction and RT-PCR as described above. Samples were analyzed for expression of known and experimentally identified candidate genes for ovarian development and function.

Laser Capture Microscopy

Ultrapure segments of mural GCs were collected from cryosectioned optimum cutting temperature-embedded ovaries containing preovulatory follicles by LCM with a Leica Laser Microdissection 6000 microscope (Leica, Wetzlar, Germany). RNA extraction and purification of the pooled mural GC samples were performed immediately after LCM using the PicoPure isolation kit (Molecular Devices, Sunnyvale, California). During purification, RNA samples were also treated on-column with RNase-free DNase I (Qiagen). RNA was then amplified (and reverse transcribed?) using Ovation RNA Amplification System V2 (NuGEN, San Carlos, California) to produce single-stranded DNA, per the manufacturer's instructions. DNA quality and sizing was determined using an Agilent Bioanalyzer 2100 (Agilent, Santa Clara, California). For microarray analysis, biotinylated DNA was hybridized with an Illumina Mouse Ref-6 whole-genome expression array, per the manufacturer's instructions (Illumina).

Generation of EBs

G4-mESCs and human amniocyte-derived induced pluripotent stem cells (hAdiPSCs)²⁸ were cultured on mouse embryonic fibroblasts (MEFs) feeder cells that were rendered mitotically inactive through irradiation. Mouse cultures were grown in mES medium: Dulbecco's modified Eagle medium (DMEM), Gibco, Carlsbad, California; 10% ES-grade HI fasting blood glucose (fetal bovine serum [FBS]), Cellgro, Manassas, Virginia; 100 U/mL ESGRO LIF, Millipore, Billerica, Massachusetts; 2 mM L-glutamine, Gibco; 0.2 mM 2-mercaptoethanol. Human colonies were cultured in hES medium: DMEM-F12, Gibco; 20% knock-out serum replacement (KOSR), Gibco; 1 mM L-glutamine, Gibco; 0.1 mM 2-mercaptoethanol, 8 ng/mL basic fibroblast growth factor, Invitrogen, Grand Island, New York.

Mature mESC colonies were detached from the feeder layer with warm 0.05% Trypsin-EDTA (Gibco); hAdiPSC colonies were detached using 1 mg/mL prewarmed collagenase IV in DMEM. Excess MEFs were removed from cell suspensions by serial plating on gelatin-coated plates before transferring the dissociated cells to low-adhesion tissue culture plates coated with 2% poly-HEMA in ethanol. Cells were cultured as a suspension in EB media (DMEM-F12, 15% KOSR, 15% HI FBS, 1 mM L-glutamine, 0.1 mM 2-mercaptoethanol, and 1% non-essential amino acids [Invitrogen, Grand Island, New York], 1% antibiotic-antimycotic solution [Invitrogen]) for a minimum of 14 days. Culture media was changed every other day

without disturbing the EBs. Aliquots of conditioned EB media were stored at -80°C for later endocrine analyses.

Ovarian Tissue and EB Comparative Microarray Analyses

Microarray experiments were designed to test the hypothesis that steroidogenic EBs would exhibit gene expression changes relevant to ovarian development and function. In order to assess differential gene expression between steroidogenic cell types and their progenitors, we performed 2 microarray comparisons using the Illumina MouseWG-6 v2.0 whole genome expression platform. The first analysis compared gene expression between the immature, developing P2 mouse ovary and the adult, isolated mural GCs to identify genes related to gonadogenesis, steroidogenesis, and hormone secretion. The second analysis compared suspended EBs to EBs that had been attached to gelatin-coated plates and underwent spontaneous steroidogenic differentiation in otherwise identical culture conditions. RNA extraction was performed for each tissue type and EB culture using commercially available kits (Qiagen), and microarray samples were assayed in biological and technical triplicates.

Ovarian microarray data were first analyzed using gene ontology and gene set enrichment analysis to identify individual genes and functional pathways that were differentially expressed in mural GCs versus the P2 ovary with an estimated false discovery rate (FDR) of less than 1%. The results were used for identification of ovarian developmental and functional candidate genes and for interpretation of subsequent comparison analyses involving steroidogenic EBs. (Gene expression data is deposited at the NCBI Gene Expression Omnibus database [accession number: GSE62565])

Both ovarian and EB microarray data were then analyzed by Ingenuity Pathway Analysis. Differential expression was considered significant when there was greater than or equal to a 2-fold change in expression with a *P* value of less than .05 and FDR of less than 10%. Comparison analysis was used to explore shared differentially regulated genes and relevant gene regulatory networks between steroidogenic EBs and ovarian tissue.

We also performed a hierarchical clustering analysis to compare genome-wide expression among ovarian tissues and EBs, computing genome-wide Pearson correlation coefficient for every pair of samples in the microarray data set. The R statistical environment was used to perform data analysis (<http://www.r-project.org/>). The microarray data were processed using the lumi package²⁹ for background subtraction, log₂ transformation, and quantile normalization. Unresponsive probes that had detected *P* values <.01 (as determined by Illumina's BeadStudio software) in less than or equal to 1 sample across all samples were removed. The remaining 25 294 probes were used for analysis. If multiple probes represent a single gene, the probe with the highest median expression across all samples was chosen to represent the expression of that gene. The final data set contained 18 029 genes. Differential expression analysis was performed using limma package.³⁰

Candidate Gene Temporal PCR Analysis and In Situ Localization

To validate the observed expression differences between P2 ovaries and adult mural GCs in our microarray experiment, 29 candidate genes relevant to gonadogenesis and steroidogenesis were evaluated by RT-PCR in each of the 4 harvested ovarian tissue samples (E9, E17, P2, 8-week adult). Primers for each gene (Table S1) were generated using Primer3 (<http://primer3.ut.ee/>), and RT-PCR reactions were run as described above.

Localization of GC candidate gene expression was assessed by in situ hybridization in paraffin-embedded, sectioned 24-week old mouse ovaries using a One-Step RT-PCR kit (Invitrogen) as previously described.³¹ Briefly, sections were dewaxed with xylene and sequentially rehydrated, then hybridized at 65°C overnight with 100 µL of probe hybridization per slide. Following hybridization, slides were washed with saline–sodium–citrate solution and Tris–NaCl–EDTA solution, incubated with α -DIG-AP antibody (Roche, Indianapolis, Indiana), and detected with BM Purple (Roche).

Embryoid body ICC

For ICC staining, EBs were dissociated and seeded onto to gelatin-coated plates as a monolayer of cells. After attachment, monolayer cultures were fixed with cold 4% paraformaldehyde/4% sucrose for 30 minutes and rinsed 3 times with phosphate-buffered saline (PBS) for 5 minutes each. The cells were blocked with 2% donkey serum, 10 mg/mL bovine serum albumin, and 1% Triton-X. Primary antibodies for ovarian markers were then applied for 2 hours at room temperature. After 3 rinses with PBS for 5 minutes each, secondary antibodies were applied. Nuclei were visualized by applying 4',6-diamidino-2-phenylindole (DAPI) for 30 minutes before a rinsing and final storage in PBS. Fluorescent microscopy was performed on a Zeiss Axiovert (Zeiss Microscopes) 40 CFL. Thirty-nine fields of view of dissociated EBs were assessed for AMHR and CYP19A1 co-expression by ICC. Primary or secondary antibodies were omitted in control samples to exclude false antigen detection due to nonspecific immunofluorescence.

Attached EB Culture and Assessment of Hormone Synthesis

Suspended EBs were transferred to gelatin-coated plates for attachment and differentiation in EB media. The hEB and mEB plating density was standardized to approximately 100 EBs per well of a 6-well tissue culture dish or 25 EBs per well of a 48-well plate. After attachment, half of the conditioned media was collected every other day and replaced with fresh EB media. Collected, conditioned media samples were stored at –80°C for later endocrine analysis.

To ensure uniform cell density during steroid hormone production analysis, EBs were dissociated with 0.05% prewarmed trypsin and the cells were reattached on gelatin-coated tissue

culture plates as a monolayer of cells at a density of 2×10^4 cells/200 µL for 96-well experiments and 6×10^4 cells/600 µL for 48-well experiments. After 3 days, the supernatant was collected and fresh EB media (control wells) or treatment media was added to the well. Treatment media contained (a) 1 mM letrozole (aromatase inhibitor), (b) 100 µM exemestane (aromatase inhibitor), (c) 5 IU/mL eCG, (d) 100 µM testosterone, or (e) 5 IU/mL eCG with 100 µM testosterone. For the remainder of the experiment, every third day (D3, 6, 9, 12 up to D15-hAdiPSCs) half of the conditioned media was collected and replaced with fresh media of the same type. Conditioned medium from the cultures was collected and stored at –80°C for later endocrine analysis. The experiments consisted of 5 repeated trials.

The E2 concentrations were assessed using commercially available enzyme-linked immunosorbent assay (ELISA) kits (Abnova, Taipei, Taiwan). These results were independently confirmed by 2 commercial endocrine laboratories (the Wisconsin National Primate Research Center and Brigham and Women's Hospital Specialty Assay Research Core) by radioimmunoassay (RIA) using biological and technical replicates. Internal standards were also performed with each round of assays. For the monolayer experiments, biological replicates were pooled from the 96-well plates in order to provide sufficient media volume for at least 2 technical replicates per experimental condition per time point. Mean E2 levels in the conditioned media of control or experimental groups were calculated and compared using a 2-tailed Student *t* test with *P* values $\leq .05$ considered statistically significant.

Fluorescence-Activated Cell Sorting

To isolate the subpopulation of steroidogenic, GC-like cells from heterogeneously differentiated EBs, we performed live fluorescence-activated cell sorting (FACS) using an antibody to the AMHR2 surface receptor. Six live FACS experiments were performed, each representing a distinct round of presort EB generation and culture. The EBs were dissociated using enzymatic digestion with cold 0.05% trypsin and by gentle pipetting and passage through a 70-µm filter to ensure single cell suspension. A modified ICC protocol was created for live ICC. The fresh single cell suspensions were blocked as described above, treated with mouse anti-AMHR2 for 1 hour on ice, washed, and treated with anti-mouse Alexa Fluor (Life Technologies/Invitrogen) 488 secondary antibody. Cell suspensions were separated into AMHR2-positive (AMHR⁺) and AMHR2-negative (AMHR⁻) fractions using a BD FACSAria multicolor high-speed sorter and FACSDiva version 6.1.2 software (BD Biosciences, Franklin Lakes, New Jersey). The AMHR⁺ and AMHR⁻ sorted cells were plated onto gelatin-coated plates cultured with EB medium at standard cell density for culture. Post-sort cultures were maintained under identical conditions for an additional week before subsequent ICC, E2 assays, RNA extraction, and RT-PCR (performed as described above.)

Bromodeoxyuridine Assay

The AMRH⁺ fraction was cultured for 24 hours to allow reattachment to gelatin-coated plates and was then cultured in EB media supplemented with 10 µg/mL bromodeoxyuridine (BrdU) for an 18-hour pulse. The cultures were then rinsed twice with PBS and given fresh EB media for another 24 hours. Fixation was performed as previously described. The cultures were permeabilized with 1 N HCl for 30 minutes and then neutralized with 0.1 N NaOH for 5 minutes. Peroxidase inactivation was performed with 0.3% H₂O₂ for 30 minutes. After blocking protocol described above, mouse anti-BrdU primary antibody (BD Biosciences) was applied for 1 hour, followed by secondary antibody for 1 hour and DAPI, as described above.

Results

Figure 1 illustrates the comparative development and maturation through folliculogenesis of vertebrate ovarian tissue *in vivo* (Figure 1A), relative to a differentiating embryonic SC model (Figure 1B). The SC colonies aggregate in suspension and under specific culture conditions differentiate to generate steroidogenic cells with subpopulations that share ovarian tissue antigenic markers. We interrogate these ESC-EB-derived steroidogenic cultures for markers of ovarian cells using ICC and PCR analysis (C); these subpopulations of ovarian antigen-expressing steroidogenic cells are then purified using FACS to demonstrate the feasibility of this system to develop an *in vitro* model for functional ovarian tissue regeneration using ESCs.

Microarray Analysis of Differential Gene Expression in mESC EBs and *In Vivo* Ovarian Tissues

In order to investigate *in vivo* transcriptional changes during ovarian development, both PCR and microarray analysis of mouse ovaries and mural GCs (Figure 2A) at different ages of development were performed. More than 1000 genes were differentially expressed between P2 ovaries and adult mural GCs. One hundred fifty-six gene sets involving 242 upregulated genes were significantly overrepresented, and 652 gene sets with 388 downregulated genes were overrepresented (Figure 2B; FDR < 1%). Many differentially expressed gene sets were related to cell cycle control, folliculogenesis, steroidogenesis, and apoptosis (Figure 2C).

Attached mEBs displayed differential gene regulation compared to their suspended counterparts and shared gene regulatory changes with both *in vivo* P2 mouse ovaries and the adult mouse mural GCs (Figure 2D and E). Three hundred eighty-two genes were differentially regulated in D3 EBs (2-fold change, FDR < 1%). Two hundred eighty-seven were upregulated, and 95 were downregulated. Top biological functions corresponded to tissue development, embryonic development, and organ development. Lipid metabolism ($P = 2E-4$), gonadogenesis ($P = 4.66E-5$), and ovarian development ($P = 2.59E-3$) were significantly overrepresented. Fourteen genes, including *Cited2*, *Ctgf*, *Fst*, *Gja1*, *Pparg*, and *Smarca1*,

were significantly enriched in both D3 EBs and mural GCs, while 59 genes, including *Dlk1*, *Gata2*, *Gli3*, *Igf2*, *MesT*, and *Sox9*, were co-enriched in P2 ovaries (Figure 2E). Estrogen receptor was predicted to serve as a key transcription regulator ($P = 2.99E-6$). Comparative analyses of suspended versus attached EBs (Figure 2E and F) demonstrated differential gene expression as seen with *in vivo* tissue, albeit with a large proportion of genes related to ESC differentiation. A subanalysis of gene expression identified changes related to emergence of steroidogenic biosynthesis (Figure 2E).

In order to demonstrate the fidelity of our microarray comparisons, we validated the expression of several known ovarian markers and candidate genes that were identified as differentially regulated in ovarian tissues and steroidogenically differentiated EBs using PCR. We created a gene expression profile related to ovarian development and function. This included assessment of known and candidate ovarian genes in E9 and E17 mouse embryos, the postnatal and mature ovary, as well as *in situ* localization of several genes of interest in ovarian follicles at multiple stages of development using adult ovarian cryosections (Figure 3 and Figure S1).

A Subset of Differentially Expressed Ovarian Genes Are Temporally and Sequentially Regulated

The PCR results show that some of the interrogated genes were expressed throughout mouse development from E9 through 8 weeks postnatal dates (Figure 3A). These genes included markers of ovarian function and development such as inhibin- α (*Inha*), inhibin β -A (*Inhb-a*), and *Foxl2*. Interestingly, other genes, such as cytochromes *Cyp7b1*, *Cyp11a1*, and *Cyp19a1*, as well as receptors for gonadotropins and estrogen, *Lhcgr*, *Esr1*, and *Esr2*, displayed a temporal expression pattern (Figure 3B). Localization of these genes in the ovarian follicle supports their likely roles in steroidogenesis and gametogenesis. The antibodies employed in this study were verified for their *in situ* ovarian follicle location using paraformaldehyde-fixed whole-mount ovarian follicle sections (Figure 4A-F).

Murine EBs Differentiate Into Steroidogenic Cells That Also Express Ovarian Tissue Antigens

Subpopulations of steroidogenic cells in mEBs immunolabeled for mature ovarian markers AMHR2, CYP19A1, and FOXL2 (Figure 5A-L). Under our differentiation conditions with extended culture, we found that our mEBs were enriched for steroidogenic cells. Of the total cells analyzed by ICC, 77% express AMHR2, 83% express CYP19A1, and 87% of these populations co-express both antigens. Overall, 72% of all cells co-expressed AMHR2 and CYP19A1. Additional genes related to ovarian development identified by microarray analysis, which were all expressed in control mouse ovary, were expressed at varying degrees in both suspended and attached mEBs (Figure 5M). Mouse lens tissue was used as a negative control and demonstrated limited expression of these genes.

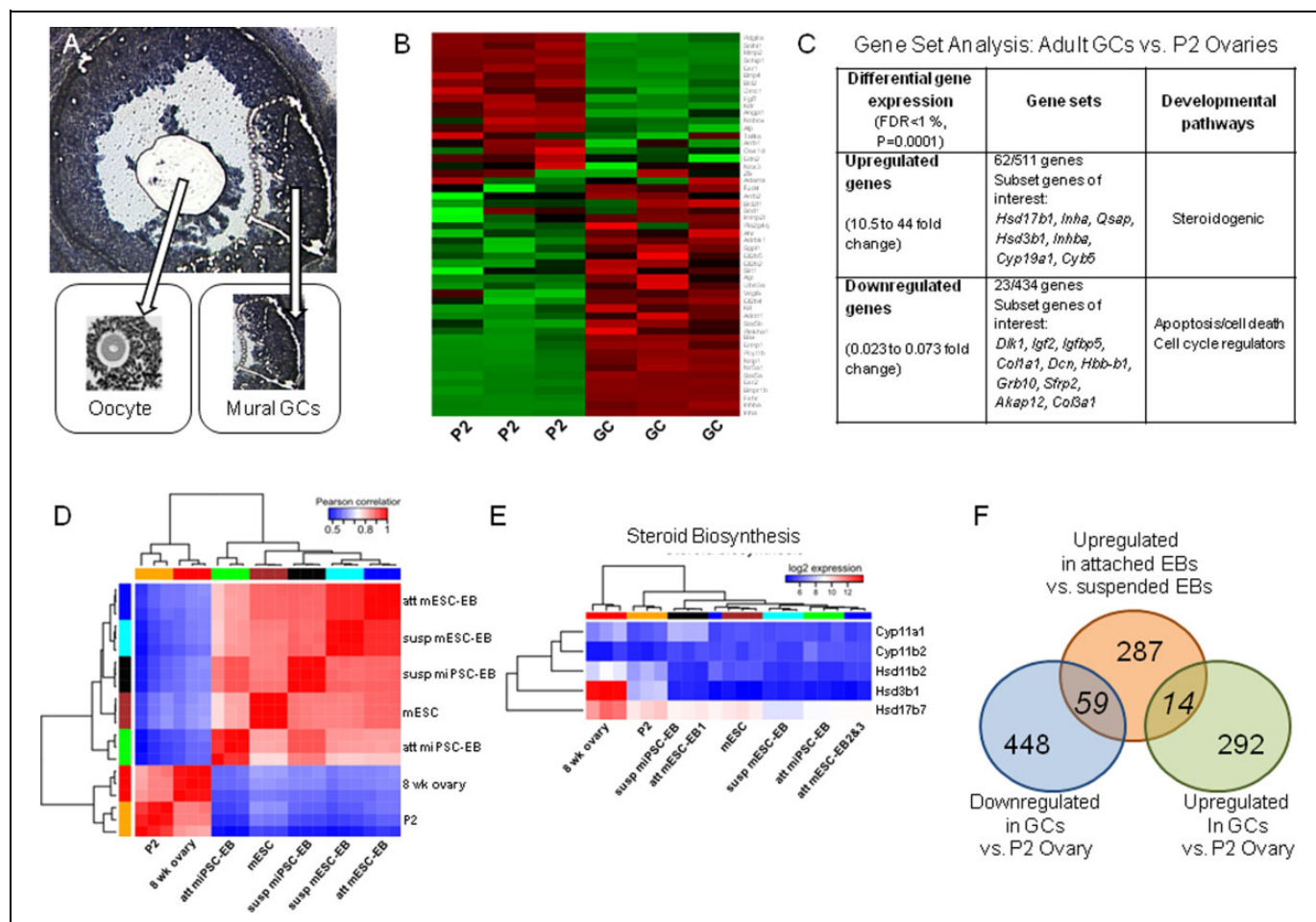


Figure 2. Microarray analysis highlighting differential gene expression patterns found in the in vitro stem cell model and in vivo ovarian tissues. Using LCM on sectioned mouse hyperstimulated ovaries, oocytes were discarded and mural GCs were circumferentially isolated and collected (A). A heat map generated by microarray data identified genes that were differentially expressed in immature, P2 ovaries, and adult mural GC (B), including those involved in relevant biological processes (C). The granulosa cell in vivo developmental gene expression profiles was compared with differential gene expression in suspended versus attached EBs with emergence of enhanced steroidogenic activity (D-F). Fourteen genes overexpressed in attached steroidogenic EBs compared to suspended EBs were also overrepresented in the isolated mural GCs compared to immature P2 ovary. Another 59 genes were underexpressed in mural GCs (F). EBs indicates embryoid bodies; GC, granulosa cell; LCM, laser capture microscopy; P2, postnatal day 2.

Differentiated mEBs Produce E2

Dissociated attached mEBs were functionally active and capable of E2 and P4 production. Attachment of EBs appears to enhance steroidogenic differentiation. The D3 attached mEBs produced significantly more E2 than D1 suspended mEBs as determined by ELISA and RIA. The E2 levels in conditioned EB media increased from D1 (30 pg/mL) to D3 (329.5 pg/mL; Figure 5N) and remained elevated through D15 of culture ($P = .002-.006$; data not shown).

Stem Cell-Derived Ovarian Granulosa-Like Cells Display Appropriate Responses to Hormone Stimulation and Inhibition

We also assessed the ability of steroidogenic EBs to convert androgens to E2 in the presence of aromatase inhibitors

(letrozole or exemestane), supplemental testosterone (T) substrate, eCG stimulation, or a combination of eCG + T as compared to control EB media alone. At baseline D0, there were no significant differences in E2 levels in conditioned media. However, after 3 days of continued culture and exposure to different media conditions (eCG, T, and eCG + T treatment; Figure 5O), we observed significant increases in E2 levels relative to controls. After 3 additional days in culture, on D6 (Figure 5O), letrozole-treated cultures produced 43% less E2 than the control culture ($P = .006$), whereas cultures treated with testosterone, eCG, and eCG + T made 85%, 96%, and 123% more than control, respectively ($P = .006$ to $3.3E-4$). Exemestane produced a paradoxical increase in E2 synthesis, producing 108% more E2 than controls by D6 of culture. The highest overall E2 levels were seen in cultures treated with eCG + T (1693 vs 759 pg/mL for control-untreated media).

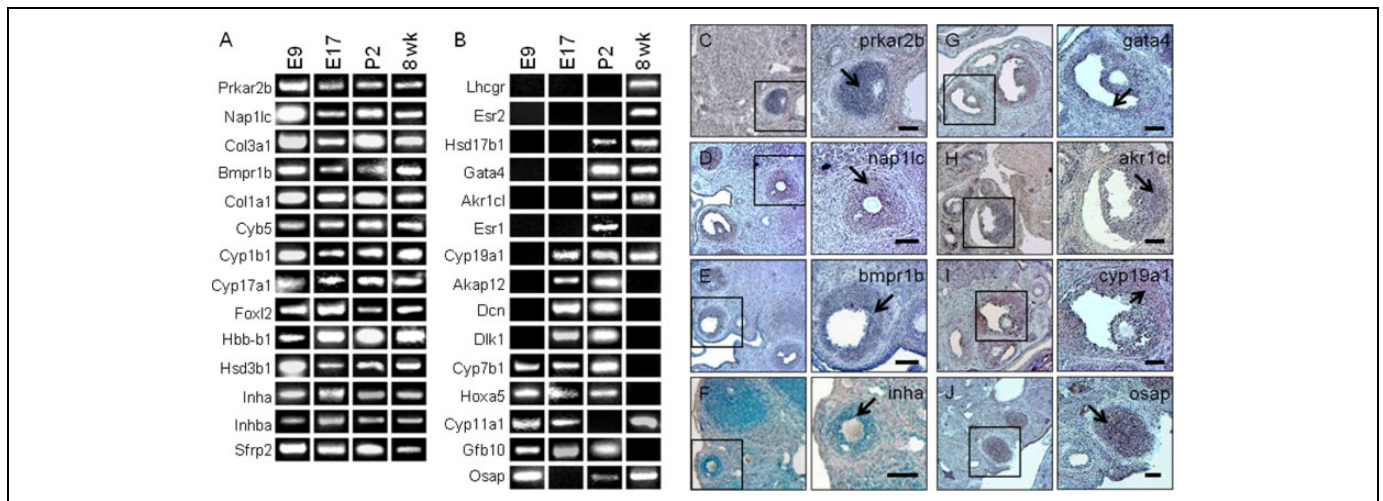


Figure 3. The RT-PCR was used to analyze a subset of genes that were differentially regulated in both the *in vitro* EB system and in the developing ovary. Microarray parameters highlighted genes with ≥ 2 -fold change in expression. Of 25 analyzed genes, 14 were actively expressed at all developmental ages (A). Fifteen genes demonstrated a temporal shift in expression-related stage of ovarian development (B). Localization of genes present in adult ovarian tissue by RT-PCR was specific to mural GCs and not found in other ovarian tissues (select examples, C-J). Scale bar: 100 μ m. EB indicates embryoid body; GCs, granulosa cells; RT-PCR, reverse transcription polymerase chain reaction.

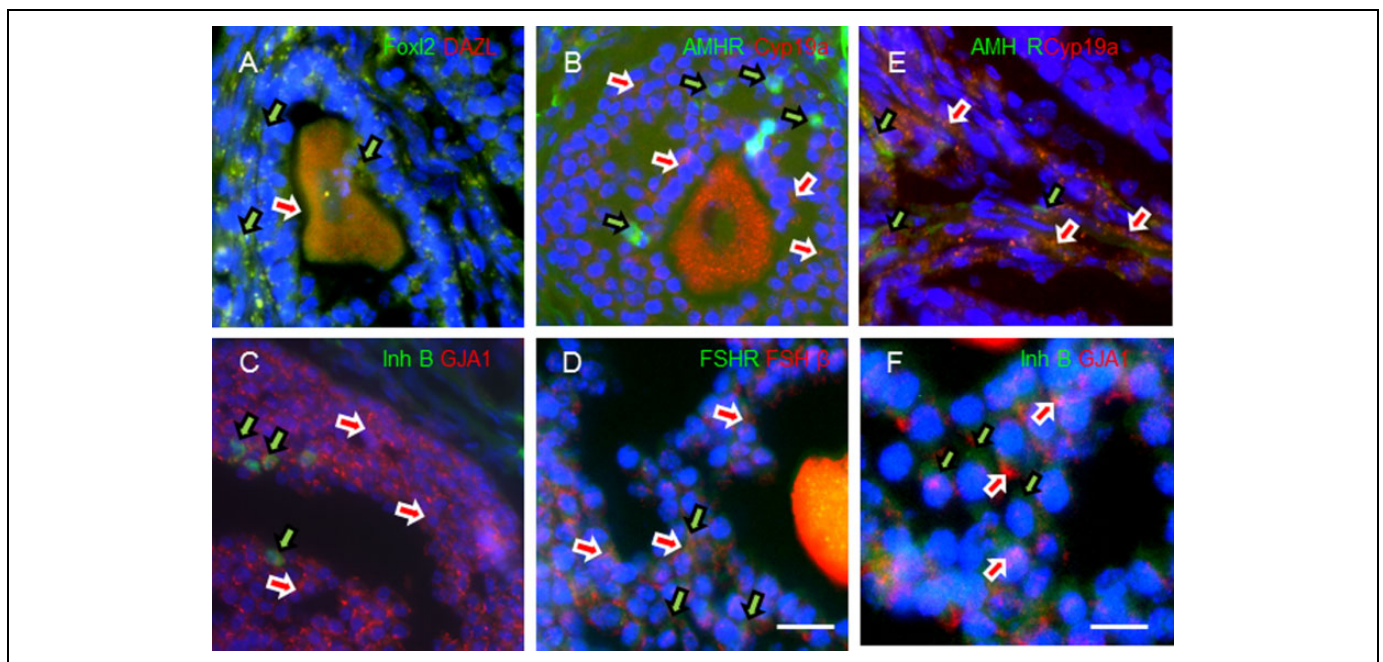


Figure 4. In order to validate antibodies used in this study, whole mount paraformaldehyde-fixed mouse ovaries were cryosectioned and immunolabeled with FOXL2/DAZL (A), AMHR2/CYP19A (B), INHB/GJA1, (C) or FSHR/FSH β (D) to demonstrate *in situ* localization of these markers within the mouse ovarian follicle (scale bar: 100 μ m). Higher magnification images showing cellular localization of AMHR2/CYP19A (E) and INHB/GJA1 (F). Scale bar: 25 μ m.

Differentiated mEBs Capable of E2 Production Can Be Purified by FACS of AMHR⁺ Cells

We used AMHR⁺ along with CYP19A1 expression as surrogate markers for identification of SC-GCs in the steroidogenic EBs and the surface marker AMHR⁺ for sorting of the desired cell population from enzymatically dissociated EBs. The

gating strategy we employed resulted in a consistent 1:4 to 1:5 ratio of AMHR⁺ to AMHR⁻ cells during 5 of 6 experiments (Figure 6A-C), with 1 experiment resulting in a lower 1:10 ratio of AMHR2⁺ to AMHR2⁻. The PCR data showed that AMHR2 was expressed in pelleted fractions that were designated as AMHR⁺ and not in those which were designated AMHR⁻ (Figure 7).

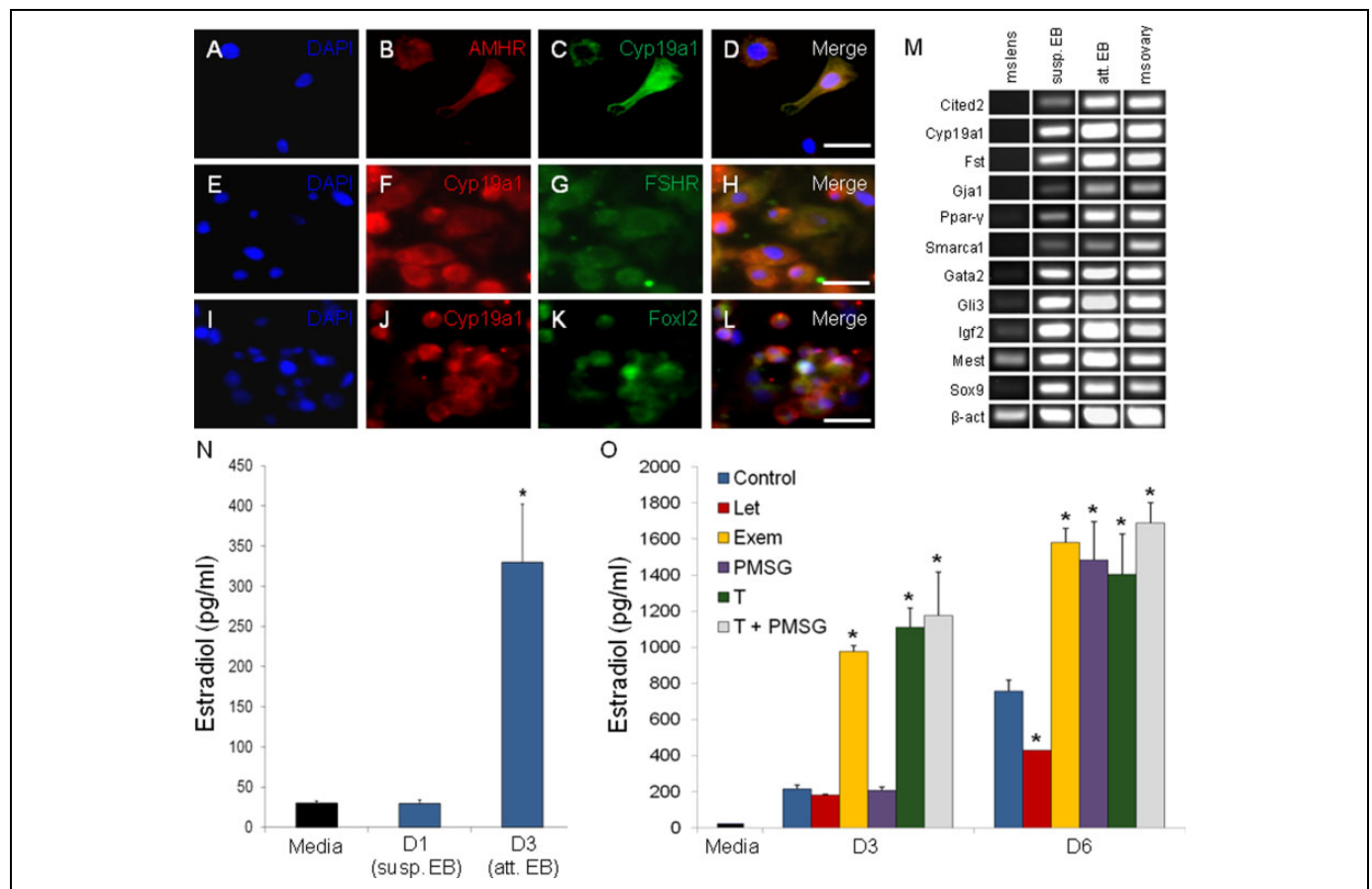


Figure 5. The in vitro EB model of ovarian development differentiates into cells that express antigens characteristic of the mature ovary, including colocalized expression of CYP19A1 with AMHR, FSHR, and FOXL2 (A–L). Expression of genes that were co-enriched in both attached EBs and adult mural GCs by microarray analysis was evaluated in suspended and attached EBs, as well as in control mouse tissues (M). Upon attachment to a gelatin substrate, EBs become steroidogenic and synthesize E2 (N). When attached EBs are treated with E2 synthesis inhibitors (letrozole, Let; exemestane, Exem), activators (eCG), and a testosterone precursor (T), the system demonstrates maintenance of steroidogenic regulatory responses (O). “Media” bar is unconditioned baseline. Exem resulted in a paradoxical increase in E2 synthesis. * $P \leq .05$. Scale bar: 25 μm . EBs indicates embryoid bodies; E2, estradiol; GCs, granulosa cells.

The AMHR⁺ sorted cells showed co-expression of *Amhr2* with *Cyp19a1* by ICC (Figure 6E–H) and also displayed expression of these and ovarian GC marker *FoxL2* by PCR (Figure 6I). Importantly, AMHR⁺ sorted cells proliferated post-sort, as evidenced by BrdU incorporation (Figure 6I–K). Three days after sorting and reattachment, AMHR⁺ cells produced significantly more E2 than AMHR⁻ sorted cells ($P \leq .03$; Figure 6J), although both populations contained cells expressing CYP19A1 by ICC. Subpopulations of AMHR⁻ sorted cells, although initially negative for AMHR2 by PCR and ICC, eventually came to demonstrate AMHR2 staining (Figure 7). Consistent with these observations, E2 levels in conditioned media from AMHR⁻ sorted cells collected 6 days after reattachment approached those of AMHR⁺ cell cultures (12 vs 14 pg/mL).

Differentiated Steroidogenic mEBs Demonstrate Expression of Ovarian GC Markers After FACS of AMHR⁺ Cells

By comparative Western blot analysis, we show that differentiated steroidogenic EBs demonstrate AMHR2, FSHR,

CYP19A1, GJA, FOXL2, and INHB protein expression comparable to GCs (Figure 7A). These results are confirmed by RT-PCR (Figure 7B). The FACS of differentiated steroidogenic mEBs was performed using the surface marker AMHR2 from enzymatically dissociated EBs as described above. As predicted, quantitative PCR (Qt-PCR) data showed trending of increased real-time expression of transcriptsomes for *Amhr2*, *Fshr*, *Cyp19a1*, *Gja1*, *Foxl2*, and *Inhb* in AMHR⁺ populations relative to AMHR⁻ (Figure 7C—Fold change on the y-axis relates to a comparison of experimental groups to the housekeeping gene β -actin. The cDNA template was omitted to generate negative control bands.) Collectively, these results suggest that an enriched population of granulosa-like cells are differentiated and purified from these steroidogenic mEBs.

Patient-Specific hAdiPSC-EBs Produce E2 and P4

The ability of hAdiPSC-EBs to generate the reproductive steroids E2 and P4 was investigated using a comparable differentiation protocol (Figure 8A–C). These differentiated hiPSC-EBs not only

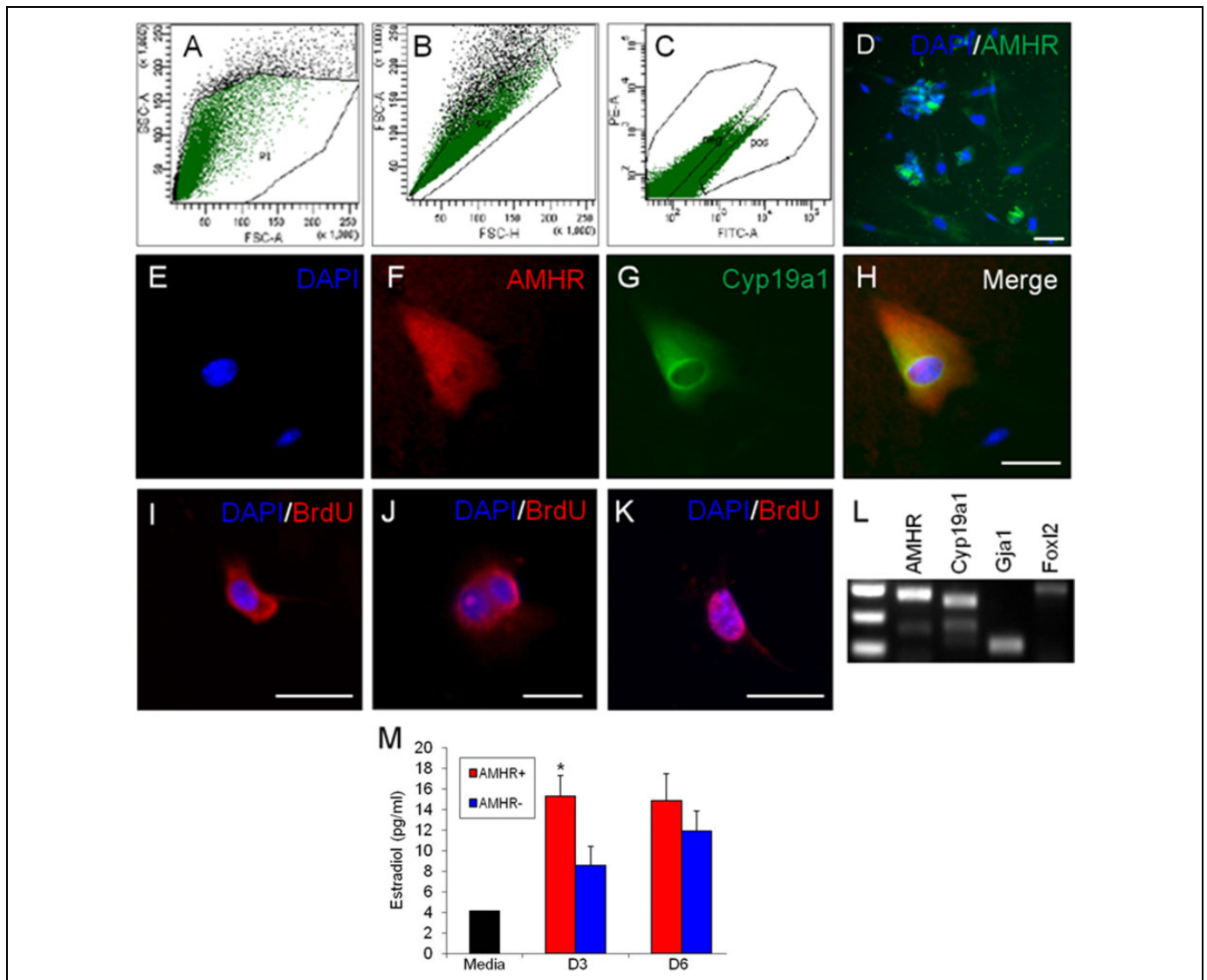


Figure 6. Stringent gates were used in live FACS of dissociated differentiated EBs (A-C), resulting in a live, purified AMHR2-expressing (AMHR⁺) cell population (D). The AMHR⁺ fraction contains cells with continued colocalized expression of granulosa cell markers AMHR and CYP19A1 after sorting (E-H). Following live FACS, the AMHR⁺ culture continued to proliferate and labeled positive for BrdU incorporation (I-K). The RT-PCR analysis also demonstrates other granulosa cell antigens are expressed in the isolated AMHR⁺ cells (L). AMHR⁺ cultures synthesize more E2 than the AMHR⁻ culture by ELISA assay (M). “Media” is unconditioned baseline. * $P \leq .05$. Scale bar: 20 μ m. DNA ladder: top band = 400 bp. BrdU indicates bromodeoxyuridine; EBs, embryoid bodies; E2, estradiol; ELISA, enzyme-linked immunosorbent assay; FACS, fluorescence-activated cell sorting; RT-PCR, reverse transcription polymerase chain reaction.

behaved in a similar manner to produce E2 and P4 but also revealed expression of the ovarian antigens AMHR2 and Cyp19a1 (Figure 8D), supporting the idea that steroidogenic hiPSC-EBs were also comprised of subpopulations of SC-GCs. By D3 post-attachment, differentiating hiPSC-EBs demonstrated steroidogenic activity (Figure 8C and D), producing physiologically relevant concentrations of E2 (58-226 pg/mL) and P4 (212-573 pg/mL) over a sustained period of 15 days in culture (Figure 9).

Discussion

Mammalian ovarian development and folliculogenesis occur through a temporally and spatially regulated series of

molecular signaling events. These culminate in steroidogenesis and gametogenesis, the 2 primary biological roles of the female ovary. The hormonal and reproductive functions of the mature ovary are carried out by ovarian follicles, each containing a single oocyte surrounded by specialized cumulus oophorus and mural GCs. Ovarian GCs are the primary site of E2 synthesis and contribute to the local follicular microenvironment. The GCs also play a critical role in the maintenance and maturation of oocytes. The dysregulation of normal GC function, whether as a consequence of abnormal development, natural ovarian aging, or environmental insults such as gonadotoxic chemotherapy, can result in POI and infertility. These problems represent a serious health burden to women, yet

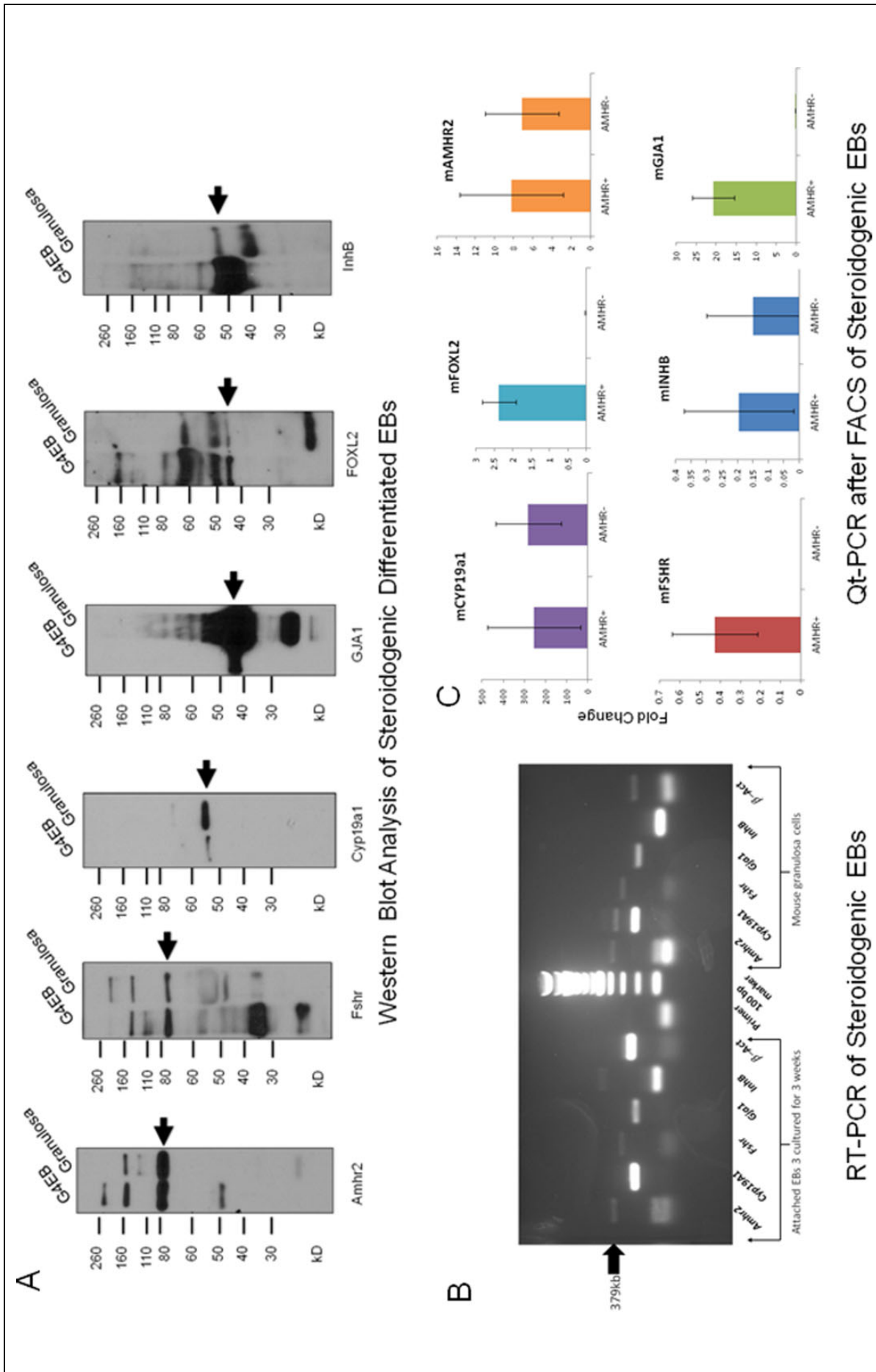


Figure 7. Comparative Western blot and RT-PCR analysis of differentiating steroidogenic EBs and granulosa cells (GCs) demonstrate comparable expression of ovarian follicular antigens. AMHR2, FSHR, CYP19A1, GJA1, FOXL2, and INHB protein expression is demonstrated in both GCs- and EB-derived steroidogenic granulosa-like cells (A). These observations are verified by RT-PCR analysis of transcriptomes from differentiating EBs relative to GC cells (B). When transcriptomes expression from purified AMHR⁺ cell populations are compared to AMHR⁻ cells, as anticipated there is a trend toward greater fold expression in the AMHR⁺ populations (C—Fold change on the y-axis relates to a comparison of experimental groups to the housekeeping gene β -actin. The cDNA template was omitted to generate negative control bands). Collectively, these data support generation of a stem cell-derived granulosa-like cell. BrdU indicates bromodeoxyuridine; EBs, embryoid bodies; RT-PCR, reverse transcription polymerase chain reaction.

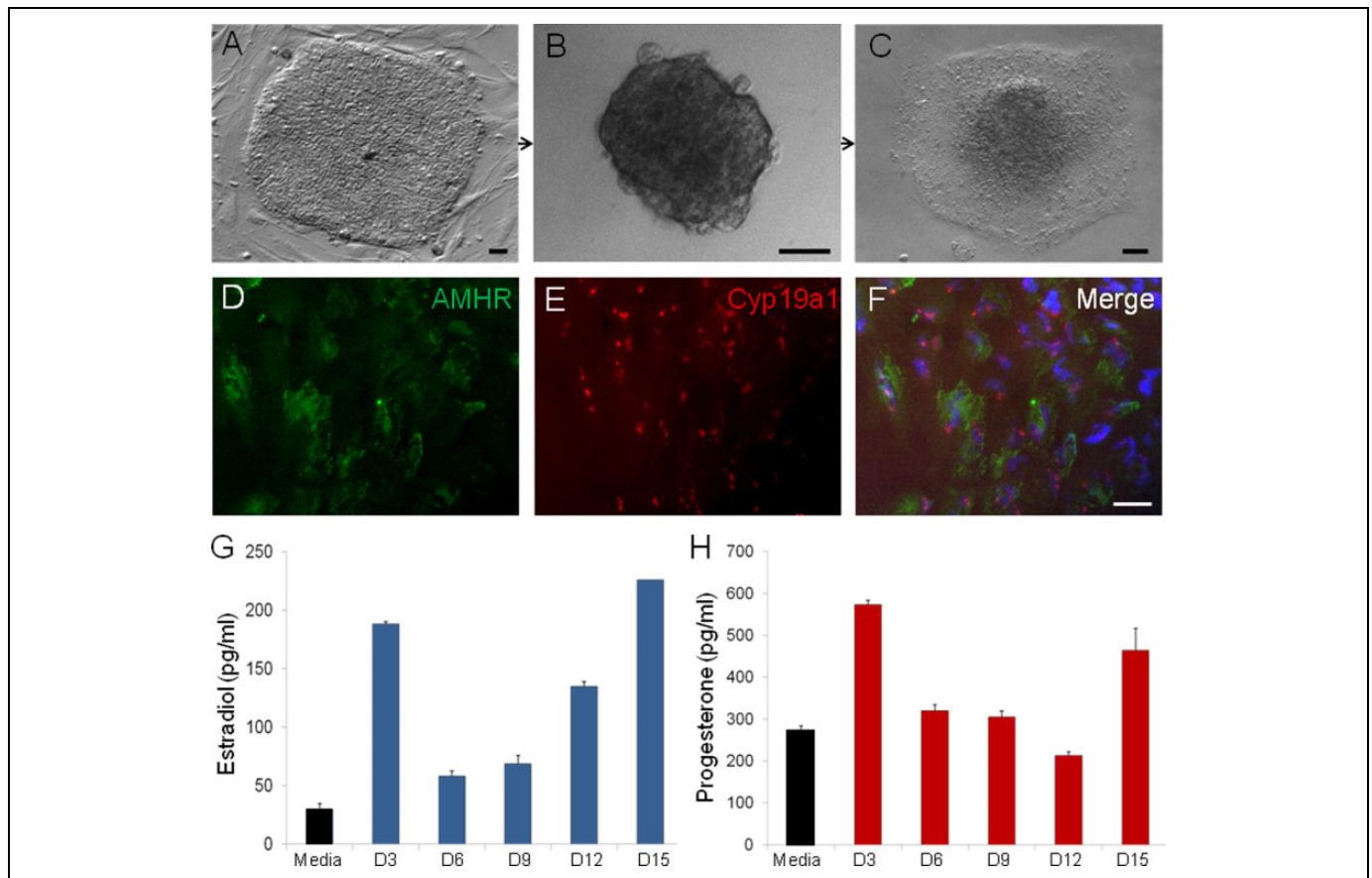


Figure 8. Human amniocyte-derived iPSCs (hAdiPSCs; A) generate hAdiPSC-EBs (B) which attach to gelatin (C) and differentiate into cell types expressing granulosa cell antigens AMHR and CYP19A1 (D-F). Over 15 days of culture, attached hAdiPSC-EBs synthesize E2 (G) and P4 (H). Scale bar: (A-C) 50 μ m and (D-F) 20 μ m. EBs indicates embryoid bodies; E2, estradiol; P4, progesterone.

current treatments (exogenous HRT and assisted reproductive technologies) and investigational methods (ovarian tissue transplantation procedures) are not without significant risks and limitations.³²⁻³⁵ Thus, there is a real need for alternative approaches, including the use of ESCs and iPSCs, to generate ovarian-like cells for in vivo and in vitro cell-based therapies.^{19,22-24} The primary findings of this report are that (1) mEBs and hEBs share a common transcriptional program with the developing ovary and (2) that these EBs are capable of gonadotropin-dependent E2 synthesis in vitro.

Several studies have examined changes in gene expression that occur during gonadal development, follicular maturation, and hormonal stimulation of mouse ovarian follicles.³⁶⁻⁴¹ Although these studies have been able to reveal genes involved in some of these processes, the key transcriptional components governing ovarian cell commitment have not been fully elucidated. It is challenging to distinguish differential gene regulation in mural GCs from that of neighboring ovarian cell types in vivo. We approached these obstacles by isolating ultrapure, functional mural GCs using LCM and, in tandem, by evaluating steroidogenic EBs as an in vitro model for GC differentiation and function. Critical analysis of gene expression during the discrete window of cellular commitment allowed us to identify

gene regulatory changes that are relevant to in vivo ovarian development and maturation.

We assessed the transcriptomes of the differentiating in vitro EBs (suspended vs attached) with those of the in vivo developing murine ovary (P2 vs adult GCs) to evaluate temporal shifts in expression in a subset of genes. Microarray analysis showed that attached, E2-synthesizing EBs displayed differential gene regulation compared to their suspended counterparts. The E2-synthesizing EBs also share distinct gene regulatory changes with both the P2 mouse ovaries and adult LCM-isolated mural GCs. Despite the heterogeneity of EB differentiation and an overrepresentation of genes related to pluripotency, several genes of interest relating to ovarian development and function emerged. Over 50% (15/29) of the developmental genes that were differentially expressed displayed temporal and sequential expression patterns between embryonic, postnatal, and mature ovarian tissues, suggesting a possible role in cell commitment and specification.

Although other studies have reported generation of GC-like cells from hESCs using BMP4, WNT3A, steroidogenic factor 1, cAMP, and activin-A supplementation^{23,42} or co-culture with ovarian cells,²² we instead identified and isolated such cells from growth factor-free, gel-adherent EB cultures. This

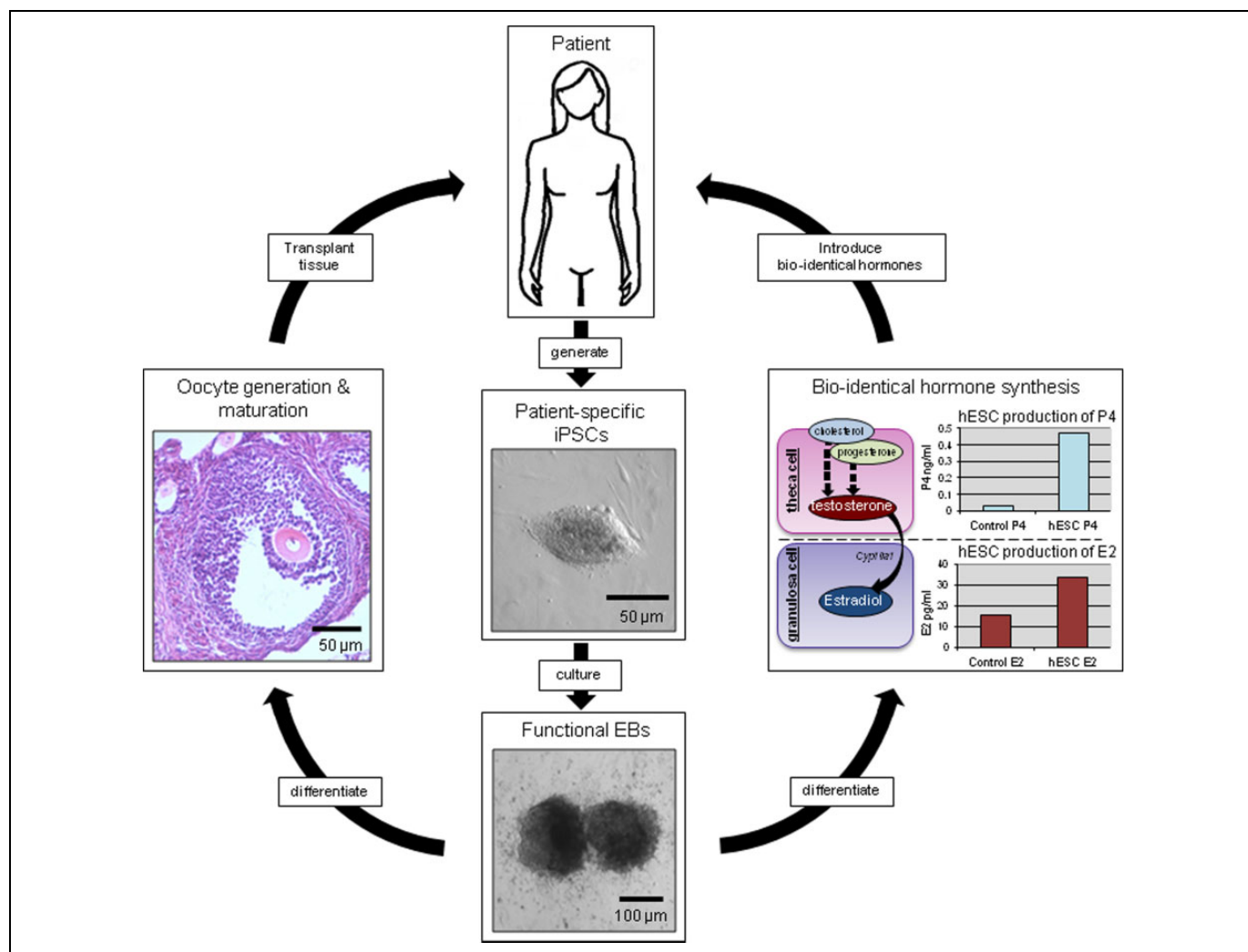


Figure 9. Proposed future applications of the in vitro stem cell model of ovarian function. Patient-specific iPSC cells would be differentiated in vitro into clinically relevant homotypic tissues, such as functional gametes and steroidogenic tissues. These antigenically matched tissues or bio-identical hormone products could be reintroduced into the originating patient to combat symptoms of ovarian dysfunction or failure. iPSC indicates induced pluripotent stem cell.

finding is significant because a minimally altered EB culture system allows for the evaluation of spontaneous, rather than exogenously induced, gene expression changes. This potentially permits more precise and biologically relevant comparisons to in vivo ovarian development and function. With this model, we are therefore able to examine the spontaneous gene regulatory changes associated with the emergence of both the primary ovarian functions: gametogenesis and steroidogenesis. Our comparative microarray analysis can serve as a starting point for future experiments in which growth factors or gene modification may be used to elaborate the roles of key developmental and functional ovarian regulators. To our knowledge, our study is the first that compares the widely used method of in vitro differentiation of EBs with in vivo ovarian development.

Our second key finding is that EB-generated steroidogenic cells not only share antigenic identity with in vivo GCs but also display appropriate responses to hormonal and pharmacologic signals. Although it is important to recognize that none of these

markers are strictly localized to ovarian GCs in vivo, collectively the co-expression and comparative pattern to GC expression provide compelling evidence that a subset of the steroidogenic cells differentiated in the EBs are granulosa-like cells. The E2 production in our EB model is enhanced by gonadotropins and testosterone and partially inhibited by the aromatase inhibitor, letrozole, relative to untreated cultures. In fact, the E2 levels produced by mEBs under our culture conditions are comparable to in vivo serum concentrations observed in cycling, reproductive-aged women. A second aromatase inhibitor, exemestane, surprisingly increased E2 synthesis. This paradoxical effect of an aromatase inhibitor has been reported previously in guinea pigs in vivo.⁴³ The capacity of our presumptive GCs to display native endocrine responses is central to future translational studies.

Importantly, there was a significant increase in steroidogenesis when differentiating EBs are attached to a substrate (in these experiments, we utilized gelatin to coat the plates). This

observation is consistent with studies that demonstrate similar results using human ESC-derived EBs attached to Matrigel.²⁵ We deliberately avoided the use of Matrigel (an EHS mouse sarcoma matrix) to better approximate *in vivo* development and decrease the risk of tumorigenesis for translational applications. The continued differentiation of steroidogenic cells with the emergence of ovarian antigens under otherwise identical culture conditions suggests that the 3-dimensional conformation of cellular aggregates may play an important role in the development of functional, tissue-specific cell types. Ongoing studies in our laboratory are further investigating this process.

Isolation of these presumptive GCs is an important step in confirming the utility of the EB model of ovarian development. In general, the heterogeneity of differentiated EBs is an obstacle to practical applications of SC-based therapies.^{22,44} The ability to isolate a purified population of the target-differentiated cells is a significant advancement toward the development of translational applications. Additionally, further characterization of the isolated cells confirms maintenance of steroidogenic functionality and a GC phenotype (CYP19A1, FOXL2, GJA1, INHB, and FSHR). We chose to use FACS for AMHR2 because it is a more specific marker of ovarian GCs than aromatase (CYP19A1), the enzyme expressed in a variety of tissues that convert androgens to E2, including nonreproductive tissues like brain,⁴⁵ bone,⁴⁶ and adipose.^{47,48}

The initial yield of sorted cells from heterogeneous differentiated EBs is low but sustainable. The presence of *Sox9* in the differentiated EB cells is consistent with evidence for early gonadal development and may indicate the presence of a precursor cell. Indeed, *Sox9* expression has been previously noted in the immature bipotential gonad as well as transiently during ovarian follicular development (Lin, Y-T and Capel, B (2015) Cell Fate commitment during mammalian sex determination. *Curr Opin Genet Dev* 32:144-152). Consistent with the notion of a precursor cell, we present evidence that the sorted cells are not only functional but also capable of ongoing growth, as demonstrated by BrdU incorporation by the dividing cells. Confirmation that the AMHR⁺ fraction is capable of continued proliferation after isolation suggests that live-FACS populations of differentiated cells provide an opportunity for clinical applications. Therefore, this system provides us with the ability to isolate a desired cell type from heterotypically differentiated ESC cultures, expand in culture, and then use for specific applications.

Patient-specific iPSCs are of vital interest to the advancement of the field of regenerative medicine and, as shown here, are able to differentiate into GC-like cells similar to those generated from mESCs. The generation of functional endocrine cells from human iPSC-derived EBs highlight the potential clinical applicability of this SC-based model for human research and translational medicine. One can foresee the possibility of using a patient's somatic cells to generate iPSCs. These could then be differentiated along the steroidogenic pathway for synthesis of bioidentical hormones or transplant of functional presumptive GCs cells into the patient (Figure 7).

Regenerated ovarian somatic cells might also be used in conjunction with assisted reproductive techniques for treatment options for infertility patients. The importance of ovarian somatic cells for oocyte development has been highlighted by successful germ cell transplantation studies in the mouse.⁴⁹ Other preliminary studies show that hESCs may organize into ovarian follicle-like structures when cultured in a 3-dimensional suspended EBs.⁵⁰ The ultimate development of a functional EB-based "artificial ovary" could have far-reaching implications for the *in vitro* maturation of oocytes harvested during ART treatments. We are pursuing additional experiments to verify that functional, GC-like cells can be generated from other human iPSC lines derived from adult somatic tissues, as the amniocytes reprogrammed in this study are only available from pregnant patients. Additional iPSC sources would expand the utility of this system.

Limitations of this study include the heterogeneity of differentiating EBs. Since there are no specific markers exclusively for GCs, it is conceivable that several other cell types sharing some of these antigens are produced. However, the collective expression of numerous GC antigens, E2 synthesis, P4 enrichment, and an isolated AMHR2-expressing population showing maintenance of antigenic and steroidogenic properties supports our conclusion that we are generating a steroidogenic granulosa-like cell in our SC culture system. Although FACS was employed to derive an enriched population of presumptive GC-like cells, the stringency of the sorting window impacts the specificity and thus purity of the sorted cells as demonstrated by the Qt-PCR results. (Note that fold change on the *y*-axis [Figure 7C] relates to a comparison of experimental groups to the housekeeping gene β -actin. The cDNA template was omitted to generate negative control bands.) The heterogeneity of the differentiating EBs also contributes to complex analyses of our LCM-microarray data and additional ongoing studies will further interrogate these results. Ultimately, transplanting these cells into an animal model to assess for follicular formation will be a necessary next step to validate this model.

Conclusion

This study demonstrates that growth factor-free, native differentiation of mEBs and hEBs can yield functional granulosa-like cells. Moreover, by using these EBs as a model for steroidogenic cell commitment, we are able to capture the gene regulatory changes that occur spontaneously upon the transition from suspended to attached culture. The availability of a model that features spontaneous differentiation of EBs into granulosa-like cells paired with *de novo* E2 synthesis provides a useful *in vitro* system for assessing the impact of specific factors, drugs, and molecules on GC differentiation and function. Our experiments also demonstrate the feasibility of isolating and expanding functional granulosa-like cells differentiated from mESC and human iPSC-derived EBs. These findings add strength to the EB model as a tool for ovarian candidate gene discovery and the elucidation of gene

regulatory networks, as well as an in vitro model of ovarian steroidogenesis.

Authors' Note

Both Shane Lipskind and Jennifer S. Lindsey contributed equally to this manuscript.

Acknowledgments

The authors would like to thank Dr Robert Barbieri for critical comments during the experimental design phase of this study and Drs Mark Hornstein and Daniel Kaser for editorial assistance.

Declaration of Conflicting Interests

The author(s) declared the following potential conflicts of interest with respect to the research, authorship, and/or publication of this article: UD is a founder of, and has an equity interest in, DxNow, a company that is developing microfluidic and imaging technologies for point-of-care diagnostic solutions, and Koek Biotech, a company that is developing microfluidic IVF technologies. These interests were reviewed and are managed by the Brigham and Women's Hospital and Partners HealthCare in accordance with their conflict of interest policies.

Funding

The author(s) disclosed receipt of the following financial support for the research, authorship, and/or publication of this article: This study is supported by NIH R01 EB015776 (UD, RLM, RMA) and NIH K12 HD001255, BWH Klarman Family Foundation New Investigator Presidential Award, the Department of OB GYN, BWH, Michael Cassidy and Caroline Wang Stem Cell Research Fund (RMA), J. Willard & Alice S. Marriott Foundation, and Peery Foundation (PP).

Supplemental Material

Supplementary material for this article is available online.

References

- Bastings L, Beerendonk CC, Westphal JR, et al. Autotransplantation of cryopreserved ovarian tissue in cancer survivors and the risk of reintroducing malignancy: a systematic review. *Hum Reprod Update*. 2019;19(5):483-506.
- Shaw JM, Bowles J, Koopman P, Wood EC, Trounson AO. Fresh and cryopreserved ovarian tissue samples from donors with lymphoma transmit the cancer to graft recipients. *Hum Reprod*. 1996; 11(8):1668-73.
- van der Stege JG, Groen H, van Zadelhoff SJ, et al. Decreased androgen concentrations and diminished general and sexual well-being in women with premature ovarian failure. *Menopause*. 2008;15(1):23-31.
- Madalinska JB, van Beurden M, Bleiker EM, et al. The impact of hormone replacement therapy on menopausal symptoms in younger high-risk women after prophylactic salpingo-oophorectomy. *J Clin Oncol*. 2006;24(22):3576-3582.
- Ahles TA, Saykin AJ. Candidate mechanisms for chemotherapy-induced cognitive changes. *Nat Rev Cancer*. 2007;7(3):192-201.
- Henderson VW. Cognitive changes after menopause: influence of estrogen. *Clin Obstet Gynecol*. 2008;51(3):618-626.
- Anasti JN, Kalantaridou SN, Kimzey LM, Defensor RA, Nelson LM. Bone loss in young women with karyotypically normal spontaneous premature ovarian failure. *Obstet Gynecol*. 1998;91(1): 12-15.
- Shapiro CL, Manola J, Leboff M. Ovarian failure after adjuvant chemotherapy is associated with rapid bone loss in women with early-stage breast cancer. *J Clin Oncol*. 2001;19(14):3306-3311.
- Kalantaridou SN, Naka KK, Papanikolaou E, et al. Impaired endothelial function in young women with premature ovarian failure: normalization with hormone therapy. *J Clin Endocrinol Metab*. 2004;89(8):3907-3913.
- Beral V, Banks E, Reeves G. Evidence from randomised trials on the long-term effects of hormone replacement therapy. *Lancet*. 2002;360(9337):942-944.
- Daly E, Vessey MP, Hawkins MM, Carson JL, Gough P, Marsh S. Risk of venous thromboembolism in users of hormone replacement therapy. *Lancet*. 1996;348(9033):977-980.
- Ross RK, Paganini-Hill A, Wan PC, Pike MC. Effect of hormone replacement therapy on breast cancer risk: estrogen versus estrogen plus progestin. *J Natl Cancer Inst*. 2000;92(4):328-332.
- Schairer C, Lubin J, Troisi R, Sturgeon S, Brinton L, Hoover R. Menopausal estrogen and estrogen-progestin replacement therapy and breast cancer risk. *JAMA*. 2000;283(4):485-491.
- Grady D, Gebretsadik T, Kerlikowske K, Ernster V, Petitti D. Hormone replacement therapy and endometrial cancer risk: a meta-analysis. *Obstet Gynecol*. 1995;85(2):304-313.
- Lacey JV Jr, Mink PJ, Lubin JH, et al. Menopausal hormone replacement therapy and risk of ovarian cancer. *JAMA*. 2002; 288(3):334-341.
- Hubner K, Fuhrmann G, Christenson LK, et al. Derivation of oocytes from mouse embryonic stem cells. *Science*. 2003; 300(5623):1251-1256.
- Novak I, Lightfoot DA, Wang H, Eriksson A, Mahdy E, Hoog C. Mouse embryonic stem cells form follicle-like ovarian structures but do not progress through meiosis. *Stem Cells*. 2006;24(8): 1931-1936.
- Chen HF, Kuo HC, Chien CL, et al. Derivation, characterization and differentiation of human embryonic stem cells: comparing serum-containing versus serum-free media and evidence of germ cell differentiation. *Hum Reprod*. 2007;22(2):567-577.
- Psathaki OE, Hubner K, Sabour D, et al. Ultrastructural characterization of mouse embryonic stem cell-derived oocytes and granulosa cells. *Stem Cells Dev*. 2011;20(12):2205-2215.
- Hayashi K, Ogushi S, Kurimoto K, Shimamoto S, Ohta H, Saitou M. Offspring from oocytes derived from in vitro primordial germ cell-like cells in mice. *Science*. 2012;338(6109):971-975.
- White YA, Woods DC, Takai Y, Ishihara O, Seki H, Tilly JL. Oocyte formation by mitotically active germ cells purified from ovaries of reproductive-age women. *Nat Med*. 2012;18(3): 413-421.
- Zhang J, Li H, Wu Z, et al. Differentiation of rat iPS cells and ES cells into granulosa cell-like cells in vitro. *Acta Biochim Biophys Sin (Shanghai)*. 2013;45(4):289-295.
- Lan CW, Chen MJ, Jan PS, Chen HF, Ho HN. Differentiation of human embryonic stem cells into functional ovarian granulosa-like cells. *J Clin Endocrinol Metab*. 2013;98(9):3713-3723.

24. Woods DC, White YA, Niikura Y, Kiatpongsan S, Lee HJ, Tilly JL. Embryonic stem cell-derived granulosa cells participate in ovarian follicle formation in vitro and in vivo. *Reprod Sci* 2013; 20(5):524-535.
25. Gerami-Naini B, Dovzhenko OV, Durning M, Wegner FH, Thomson JA, Golos TG. Trophoblast differentiation in embryoid bodies derived from human embryonic stem cells. *Endocrinology*. 2004;145(4):1517-1524.
26. Guven S, Lindsey JS, Poudel I, et al. Functional maintenance of differentiated embryoid bodies in microfluidic systems: a platform for personalized medicine. *Stem Cells Transl Med*. 2015; 4(3):261-268.
27. Anchan RM, Gerami-Naini B, Lindsey JS, et al. Efficient differentiation of steroidogenic and germ-like cells from epigenetically-related iPSCs derived from ovarian granulosa cells. *PLoS One*. 2015;10(3):e0119275.
28. Anchan RM, Quaas P, Gerami-Naini B, et al. Amniocytes can serve a dual function as a source of iPSCs and feeder layers. *Hum Mol Genet*. 2011;20(5):962-974.
29. Du P, Kibbe WA, Lin SM. lumi: a pipeline for processing Illumina microarray. *Bioinformatics*. 2008;24(13):1547-1548.
30. Smyth GK. Linear models and empirical Bayes methods for assessing differential expression in microarray experiments. *Stat Appl Genet Mol Biol*. 2004;3:Article3.
31. Sassoon D, Rosenthal N. Detection of messenger RNA by in situ hybridization. *Methods Enzymol*. 1993;225:384-404.
32. Narod SA. Hormone replacement therapy and the risk of breast cancer. *Nat Rev Clin Oncol*. 2011;8(11):669-676.
33. Beral V, Reeves G, Bull D, Green J, Million Women Study C. Breast cancer risk in relation to the interval between menopause and starting hormone therapy. *J Natl Cancer Inst*. 2011;103(4):296-305.
34. Hovatta O. Methods for cryopreservation of human ovarian tissue. *Reprod Biomed Online*. 2005;10(6):729-734.
35. Shaw J, Trounson A. Oncological implications in the replacement of ovarian tissue. *Hum Reprod*. 1997;12(3):403-405.
36. Uda M, Ottolenghi C, Crisponi L, et al. Foxl2 disruption causes mouse ovarian failure by pervasive blockage of follicle development. *Hum Mol Genet*. 2004;13(11):1171-1181.
37. Ottolenghi C, Omari S, Garcia-Ortiz JE, et al. Foxl2 is required for commitment to ovary differentiation. *Hum Mol Genet*. 2005; 14(14):2053-2062.
38. Yoon SJ, Kim KH, Chung HM, et al. Gene expression profiling of early follicular development in primordial, primary, and secondary follicles. *Fertil Steril*. 2006;85(1):193-203.
39. Dharma SJ, Modi DN, Nandedkar TD. Gene expression profiling during early folliculogenesis in the mouse ovary. *Fertil Steril*. 2009;91(suppl 5):2025-2036.
40. Hasegawa A, Kumamoto K, Mochida N, Komori S, Koyama K. Gene expression profile during ovarian folliculogenesis. *J Reprod Immunol*. 2009;83(1-2):40-44.
41. Irie N, Weinberger L, Tang WW, et al. SOX17 is a critical specifier of human primordial germ cell fate. *Cell*. 2015;160(1-2): 253-268.
42. Jadhav U, Jameson JL. Steroidogenic factor-1 (SF-1)-driven differentiation of murine embryonic stem (ES) cells into a gonadal lineage. *Endocrinology*. 2011;152(7):2870-2882.
43. Choate JV, Resko JA. Paradoxical effect of an aromatase inhibitor, CGS 20267, on aromatase activity in guinea pig brain. *J Steroid Biochem Mol Biol*. 1996;58(4):411-415.
44. Darabi R, Gehlbach K, Bachoo RM, et al. Functional skeletal muscle regeneration from differentiating embryonic stem cells. *Nat Med*. 2008;14(2):134-143.
45. Naftolin F, Ryan KJ, Petro Z. Aromatization of androstenedione by the anterior hypothalamus of adult male and female rats. *Endocrinology*. 1972;90(1):295-298.
46. Sasano H, Uzuki M, Sawai T, et al. Aromatase in human bone tissue. *J Bone Miner Res*. 1997;12(9):1416-1423.
47. Meseguer A, Puche C, Cabero A. Sex steroid biosynthesis in white adipose tissue. *Horm Metab Res*. 2002;34(11-12): 731-736.
48. Belanger C, Luu-The V, Dupont P, Tchernof A. Adipose tissue intracrinology: potential importance of local androgen/estrogen metabolism in the regulation of adiposity. *Horm Metab Res*. 2002;34(11-12):737-745.
49. Niikura Y, Niikura T, Tilly JL. Aged mouse ovaries possess rare premeiotic germ cells that can generate oocytes following transplantation into a young host environment. *Aging (Albany NY)*. 2009;1(12):971-978.
50. Aflatoonian B, Ruban L, Jones M, Aflatoonian R, Fazeli A, Moore HD. In vitro post-meiotic germ cell development from human embryonic stem cells. *Hum Reprod*. 2009;24(12): 3150-3159.